

ON THE EFFICIENT IMPLEMENTATION OF THE CAPON SPECTRAL ESTIMATOR

Torbjörn Ekman¹

Signals and Systems Group, Uppsala University
Box 528, SE-751 20 Uppsala, SWEDEN
e-mail: torbjorn.ekman@signal.uu.se

Andreas Jakobsson, Petre Stoica

Systems and Control Group, Uppsala University
Box 27, SE-751 03 Uppsala, SWEDEN

ABSTRACT

We present an efficient implementation of the Amplitude Spectrum Capon (ASC) estimator. The implementation is based on the FFT and an efficient computation of the Cholesky-factor for the inverse covariance matrix. The Cholesky-factor is obtained from the linear prediction coefficients as computed by the modified covariance method. The implementation is significantly simpler than previous implementations, and it will yield spectral estimates of a similar quality as these. A short discussion on the differences between different Capon estimators is also included.

1. INTRODUCTION

There has of lately been an increased interest in *non-parametric* spectral estimation, in particular using the Power Spectrum Capon (PSC) and the Amplitude Spectrum Capon (ASC) estimators. An important difference between these estimators is that the ASC estimator gives a least-squares (LS) estimate of the amplitude and the phase of a complex-valued sinusoid located at the frequency of interest, whereas the PSC estimator, ignoring the noise, estimate the power of the Capon filter output, and is thus not yielding an estimate of the phase information [1]. This is one of the PSC estimator's major drawbacks as the phase information is often desired in applications.

In this work we present a computationally efficient implementation of the ASC spectral estimation algorithm, termed MASC, which is based on an efficient estimation of the Cholesky factor of the inverse covariance matrix. The proposed estimate of the Cholesky factor depends only on the linear prediction coefficients (LPC) and the prediction error variance sequence, which both are obtained from Marple's fast implementation of the modified covariance method (MCM) [2]. The presented spectral estimator takes full account of the highly structured problem formulation, and can be implemented using the Fast Fourier Transform (FFT). The

proposed algorithm has close connections to both the efficient ASC implementation presented by Liu *et al* [3] and the efficient PSC implementation presented by Musicus [4]. The difference between our implementation and that of Liu *et al* is that in the Liu *et al* implementation the Cholesky factor of the inverse covariance matrix is found from the sample-covariance matrix, as opposed to in our method where the Cholesky factor is directly estimated from the data using estimated LPCs. The PSC spectral estimate in [4] is also based on LPCs, although an important difference between this approach and ours is that the LPCs are there estimated using the Levinson-Durbin algorithm (see, e.g., [5, 6]), whereas our implementation is based on the MCM. It is well known that the autoregressive (AR) spectral estimates obtain by using the MCM algorithm will have higher resolution than the AR estimates obtained from the solution to the Yule-Walker equations [2]. The same will also hold for the Capon estimators. Another difference is of course that our method yields an ASC estimate, whereas the algorithm in [4] yields a PSC estimate.

The paper is organized as follows. In the next section the ASC and the PSC spectral estimators are briefly reviewed. Then, in Section 3, the computationally efficient ASC algorithm is presented. Finally, Section 4 contains some illustrative numerical examples.

2. THE ASC AND THE PSC ESTIMATORS

In the filterbank approach to spectral estimation, the spectrum is estimated by passing the signal through a L -tap narrowband filter, \mathbf{h}_ω , with varying center frequency ω (see, e.g., [7, 8]). The filter \mathbf{h}_ω is designed to pass ω undistorted. Here, and in the following, the subscript ω is used to indicate a dependence on the filter's center frequency.

Let $\{x(n); n = 0, \dots, N - 1\}$ denote the available (stationary) data sample of which the spectrum is to be estimated. The filter output can then be written as

$$\mathbf{h}_\omega^H \mathbf{y}(t) = \alpha_\omega e^{i\omega t} + \epsilon(t), \quad (1)$$

for $t = 0, \dots, M - 1$, where $\mathbf{y}(t)$ is the forward data vector

$$\mathbf{y}(t) = [x(t) \quad \dots \quad x(t + L - 1)]^T, \quad (2)$$

This work was supported by the Swedish Foundation for Strategic Research and the Swedish National Board for Industrial and Technical Development.

¹ T. Ekman is currently on leave at the Group for Data Analysis, Signal and Image Processing, Oslo University, Box 1080 Blindern, 0316 Oslo, Norway.

and where $(\cdot)^T$ and $(\cdot)^H$ denote transpose and complex conjugate transpose, and $\epsilon(t)$ is some additive colored noise. Here, $M = N - L + 1$, is the number of subvectors. In the following we assume that $\epsilon(t)$ is uncorrelated with $\alpha_\omega e^{i\omega t}$. This assumption is basically only true for spectral lines, although it has been found to be a reasonable approximation in other cases as well [7].

The LS estimate of the complex amplitude, α_ω , in (1) is given by

$$\hat{\alpha}_\omega = \mathbf{h}_\omega^H \mathbf{Y}_\omega, \quad (3)$$

where

$$\mathbf{Y}_\omega = \frac{1}{M} \sum_{t=0}^{M-1} \mathbf{y}(t) e^{-i\omega t}. \quad (4)$$

The Capon filter [9] is given by

$$\mathbf{h}_\omega = \hat{\mathbf{R}}_y^{-1} \mathbf{a}_\omega(L) \left(\mathbf{a}_\omega^H(L) \hat{\mathbf{R}}_y^{-1} \mathbf{a}_\omega(L) \right)^{-1}, \quad (5)$$

where

$$\mathbf{a}_\omega(L) = [1 \quad e^{i\omega} \quad \dots \quad e^{i(L-1)\omega}]^T, \quad (6)$$

is the Fourier vector, and $\hat{\mathbf{R}}_y$ is an estimate of the covariance matrix of $\mathbf{y}(t)$, i.e.,

$$\mathbf{R}_y = E \{ \mathbf{y}(t) \mathbf{y}(t)^H \}, \quad (7)$$

where $E \{ \cdot \}$ denotes expectation. The ASC estimate, at frequency ω , is given by (3) evaluated using the filter (5), i.e.,

$$\hat{\alpha}_\omega^{ASC} = \mathbf{h}_\omega^H \mathbf{Y}_\omega = \frac{\mathbf{a}_\omega^H(L) \hat{\mathbf{R}}_y^{-1} \mathbf{Y}_\omega}{\mathbf{a}_\omega^H(L) \hat{\mathbf{R}}_y^{-1} \mathbf{a}_\omega(L)}, \quad (8)$$

and the spectral estimate is the magnitude square of (8), i.e.,

$$\hat{\varphi}_\omega^{ASC} = |\hat{\alpha}_\omega^{ASC}|^2. \quad (9)$$

The PSC spectral estimator is obtained by estimating the power of the filter output, i.e.,

$$\begin{aligned} \hat{\varphi}_\omega^{PSC} &= \frac{1}{M} \sum_{t=0}^{M-1} |\mathbf{h}_\omega^H \mathbf{y}(t)|^2 = \mathbf{h}_\omega^H \hat{\mathbf{R}}_y \mathbf{h}_\omega \\ &= \frac{1}{\mathbf{a}_\omega^H(L) \hat{\mathbf{R}}_y^{-1} \mathbf{a}_\omega(L)}. \end{aligned} \quad (10)$$

By ignoring the additive noise term, $\epsilon(t)$, in (1), the PSC estimator can be seen as an estimate of $|\hat{\alpha}_\omega|^2$. Note that ASC, as it does account for the noise, in general will yield a different, and often preferable, spectral estimate than the PSC spectral estimator.

3. PROPOSED EFFICIENT IMPLEMENTATION

The product between the Fourier vectors and the inverse covariance matrix in (8) and (10) can, with a Cholesky factorization of the inverse covariance matrix, be efficiently calculated using the FFT [3, 8]. Let

$$\mathbf{C} \triangleq \hat{\mathbf{R}}_y^{-1/2} \quad (11)$$

denote a square root of the positive definite matrix $\hat{\mathbf{R}}_y^{-1}$, so that $\mathbf{C}\mathbf{C}^H = \hat{\mathbf{R}}_y^{-1}$, and let

$$\boldsymbol{\nu}_\omega = \mathbf{C}^H \mathbf{a}_\omega(L) \quad (12)$$

$$\boldsymbol{\mu}_\omega = \mathbf{C}^H \mathbf{Y}_\omega = \frac{1}{M} \mathbf{C}^H \mathbf{W} \mathbf{a}_\omega^*(M), \quad (13)$$

where

$$\mathbf{W} = [\mathbf{y}(1) \quad \dots \quad \mathbf{y}(M)]. \quad (14)$$

Here, $(\cdot)^*$ is used to denote the complex conjugate. The vectors $\boldsymbol{\nu}_\omega$ and $\boldsymbol{\mu}_\omega$ can be efficiently calculated for all frequencies on the frequency grid using the FFT. A column wise FFT of \mathbf{C} gives all the $\boldsymbol{\nu}_\omega^H$, whereas a row wise FFT of $\mathbf{C}^H \mathbf{W} / M$ gives $\boldsymbol{\mu}_\omega$ for all the frequencies considered. Making use of (10), as well as (12), the PSC spectral estimate can be formulated as

$$\hat{\varphi}_\omega^{PSC} = \frac{1}{\boldsymbol{\nu}_\omega^H \boldsymbol{\nu}_\omega}. \quad (15)$$

Similarly, the ASC spectral estimate is found as in (9), where the complex amplitude estimates can be formulated as (see [1, 8] for further details)

$$\hat{\alpha}_\omega^{ASC} = \frac{\boldsymbol{\nu}_\omega^H \boldsymbol{\mu}_\omega}{\boldsymbol{\nu}_\omega^H \boldsymbol{\nu}_\omega}. \quad (16)$$

Thus, both the PSC and the ASC spectral estimators can, given an estimate of \mathbf{C} , be efficiently computed using the FFT.

Both the classical ASC and PSC implementations and the recently proposed implementations by Liu *et al* can use either an estimate of the forward-only outer-product covariance matrix (F-ASC and F-PSC), i.e.,

$$\hat{\mathbf{R}}_y^F = \frac{1}{M} \sum_{t=0}^{M-1} \mathbf{y}(t) \mathbf{y}(t)^H = \frac{1}{M} \mathbf{W} \mathbf{W}^H, \quad (17)$$

or an estimate of the forward-backward averaged covariance matrix (FB-ASC and FB-PSC), i.e.,

$$\hat{\mathbf{R}}_y^{FB} = \frac{1}{2} \left(\hat{\mathbf{R}}_y^F + \mathbf{J} (\hat{\mathbf{R}}_y^F)^T \mathbf{J} \right), \quad (18)$$

where \mathbf{J} is the exchange matrix whose anti-diagonal elements are ones and all other elements are zero, to compute the estimates in (9) or (10). The Liu *et al* implementations will thus be computationally unnecessarily cumbersome, as they requires the computing of an estimate of the covariance matrix, as the product of two $L \times M$ matrixes, as well as a Cholesky factorization and the inversion of a matrix of size L to get \mathbf{C}^H .

Here, we instead propose to compute the ASC estimate in (16) by constructing \mathbf{C} directly from the forward prediction coefficients (see, e.g., [2], Chapter 3.8)

$$\mathbf{C} = \begin{bmatrix} 1 & 0 & \dots & 0 \\ a_{L-1}(1) & 1 & & \vdots \\ \vdots & \ddots & \ddots & \\ a_{L-1}(L-1) & a_1(1) & 1 & \end{bmatrix} \begin{bmatrix} \sigma_{L-1}^{-1} & 0 & \dots & 0 \\ 0 & \sigma_{L-2}^{-1} & & 0 \\ \vdots & \ddots & \ddots & \vdots \\ 0 & \dots & 0 & \sigma_0^{-1} \end{bmatrix} \quad (19)$$

where $a_p(k)$ denotes the k th (forward) LPC of order p , satisfying

$$e_p(n) = x(n) + \sum_{k=1}^p a_p(k)x(n-k), \quad (20)$$

and σ_p is the prediction error standard deviation of model order p , i.e.,

$$\sigma_p = \sqrt{E\{|e_p(n)|^2\}}. \quad (21)$$

The needed LPCs in (19) can be computed in numerous ways. We will in the following use the MCM, as it will produce spectral estimates with higher resolution than, for instance, the solution to the Yule-Walker equations would. Thus, we term the resulting ASC estimator, as obtained by combining (16) and (19), the MASC estimator². It is worth stressing that by estimating the AR coefficients using the MCM one avoids the problem of line-splitting and frequency bias that would occur if, e.g., the Burg algorithm was used instead [2]. The MCM algorithm estimates the LPCs directly from data and does not need to calculate a covariance estimate first.

4. NUMERICAL EXAMPLES

The true spectrum of the simulation data, as seen in Figure 1, consists of three dominant spectral lines and ten smaller spectral lines located at the following normalized frequencies: 0.062, f_2 , 0.25, 0.28, 0.33, 0.35, 0.37, 0.39, 0.41, 0.43, 0.45, 0.47, 0.49. The second spectral line, located at f_2 , is in the following varied to demonstrate the resolution properties of the estimators. The spectral lines all have a phase value of $\pi/4$. The data sequence has $N = 64$ data samples and is corrupted by complex white Gaussian noise with zero mean and variance σ^2 . The SNR for a spectral line is defined as $10\log_{10}(|\alpha_\omega|^2/\sigma^2)$ [dB].

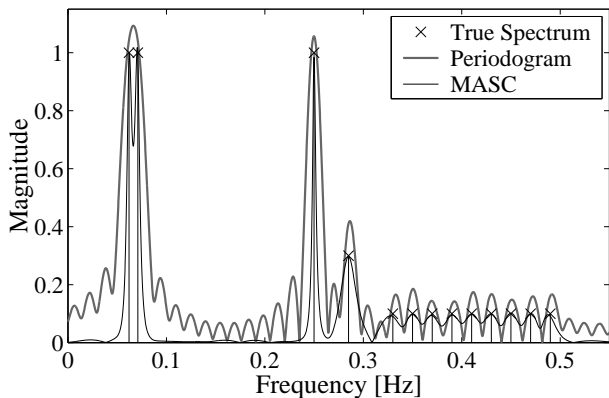


Figure 1: The true magnitude spectrum, with the second line at $f_2 = 0.071$, the Periodogram and the MASC estimate.

² A MATLAB implementation of the MASC estimator is available upon request from the first author.

First we study the different spectral estimators' resolution by varying the location of the second spectral line. Let $\hat{\varphi}_\omega$ denote an amplitude spectral estimate at frequency ω . One can then consider the two sinusoidal signals resolved if $\gamma = 2\hat{\varphi}_{\omega_3} - \hat{\varphi}_{\omega_1} - \hat{\varphi}_{\omega_2} < 0$, where ω_3 is the midway frequency between ω_1 and ω_2 . Figure 2 shows the resolution ability of the ASC and the PSC spectral estimators as compared to the standard Periodogram. As seen from the figure the resolution curves for the MASC and the FB-ASC estimators coincide, both having slightly lower resolution than the F-ASC. It is worth noting that the ASC methods will have significantly higher resolution than both the PSC methods and the Periodogram³. Here, the SNR = 30 dB for the two first lines. Unless otherwise stated, the used filter is $L=16$ taps long and the results are obtained from 500 Monte Carlo trials.

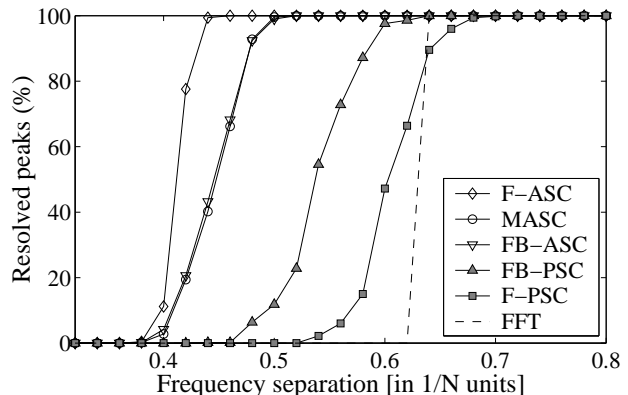


Figure 2: Resolution limits when the second peak is varied.

We proceed by comparing the mean squared error (MSE) of the power spectral estimates (the magnitude squared amplitude spectral estimate) for the different estimators. Figure 3 shows how the MSE of the power spectral estimates varies for the FB-ASC, FB-PSC, MASC estimators and the Periodogram as the second spectral line is moved (SNR = 20 dB). As seen in the figure, the MASC estimator shows less of a dependency on the frequency separation of the spectral lines as compared to the FB-ASC estimator (the forward-only estimators perform worse than their forward-backward counterparts) and is thus found to yield a more reliable power spectral estimate.

Figure 4 compares the MSE of the power spectral estimates for the second spectral line, separated $2/N$ from the first, for the F-ASC, FB-ASC, MASC, FB-PSC estimators as well as for the Periodogram. The MASC estimate is seen to yield a superior estimate as compared to the other methods. If instead the line separation would have been $2.5/N$ the difference in performance would have been smaller (as seen in Figure 3).

Finally, Figure 5 illustrates the relative computational

³ In fact, in [10] it was found that the ASC methods have higher resolution than even the *parametric* MUSIC estimator, which assumes full knowledge of the data structure.

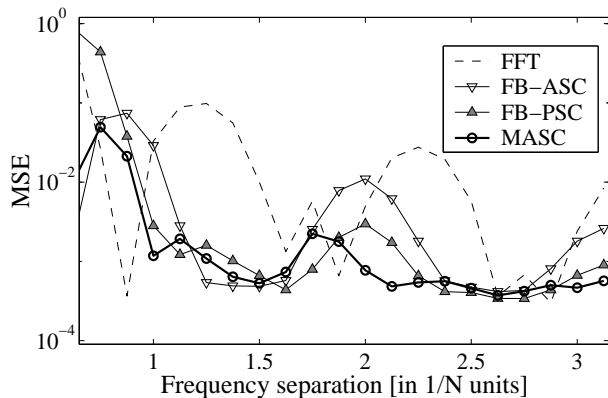


Figure 3: The MSE of the power spectral estimate for the second peak, as the separation of the peaks varies.

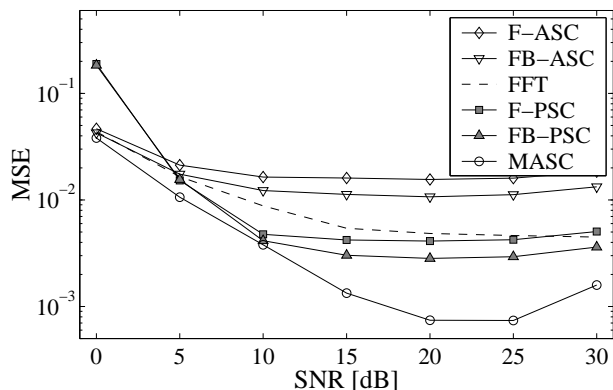


Figure 4: The MSE of the power spectral estimate of the second peak.

complexity of the different ASC and PSC implementations as the data length, N , varies. Note that the F and FB spectral estimators have almost the same computational complexity as they differ only in the summation of the forward and backward covariance matrix (18). The computational load for the FB-ASC and FB-PSC are obtained by using the Cholesky based implementation by Liu *et al* (the classical implementations are significantly more cumbersome). In the figure, the estimators' computational load, as measured by MATLAB, has for clarity of presentation been normalized with the load of the MASC method. In the example, the filterlength was $L = N/4$, and the spectrum was evaluated for $4N$ grid-points (to obtain a sufficiently high resolution). The only difference between our method and the method presented in Liu *et al* is how the Cholesky factor is calculated. The remaining computations are the same. For $N = 256$, the direct calculation of the forward-backward covariance, the Cholesky factorization and its inverse amounts to roughly 54% of the total number of floating point operations (flops) as compared to about 4% in our approach. It is worth noting that a direct calculation of the FB-ASC using (8) (not exploiting the Cholesky decomposition) would, for $N = 256$, render about 15 times more computations than the MASC method.

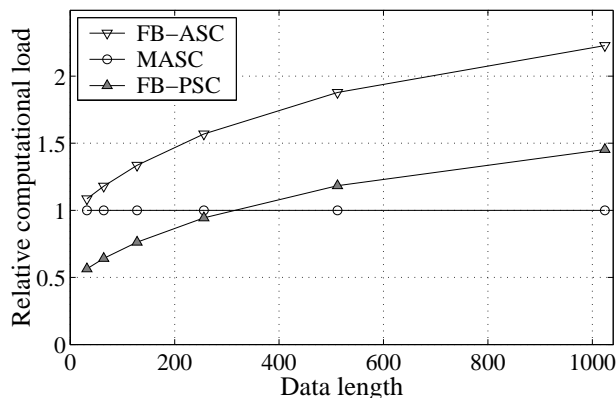


Figure 5: Relative computational complexity vs data length.

5. REFERENCES

- [1] A. Jakobsson, *Model-Based and Matched-Filterbank Signal Analysis*, PhD thesis, Uppsala University, Uppsala, Sweden, 2000.
- [2] S.L. Marple, Jr., *Digital Spectral Analysis*, Prentice-Hall, Englewood Cliffs, N.J., 1987.
- [3] H. Li Z.-S. Liu and J. Li, Efficient implementation of capon and APES for spectral estimation, *IEEE Trans. on Aero. and Elec. Syst.*, **34**(4):1314–1319, October 1998.
- [4] B. Musicus, Fast MLM power spectrum estimation from uniformly spaced correlations, *IEEE Trans. on ASSP*, **33**(4):1333–1335, October 1985.
- [5] P. Stoica and R. Moses, *Introduction to Spectral Analysis*, Prentice Hall, Upper Saddle River, NJ, 1997.
- [6] T. Söderström and P. Stoica, *System Identification*, Prentice Hall International, London, UK, 1989.
- [7] J. Li and P. Stoica, Adaptive filtering approach to spectral estimation and SAR imaging, *IEEE Trans. on Sig. Proc.*, **44**(6):1469–1484, June 1996.
- [8] P. Stoica, A. Jakobsson, and J. Li, Matched-filter bank interpretation of some spectral estimators, *Signal Processing*, **66**(1):45–59, April 1998.
- [9] J. Capon, “High Resolution Frequency Wave Number Spectrum Analysis”, *Proc. IEEE*, **57**:1408–1418, 1969.
- [10] A. Jakobsson and P. Stoica, Combining Capon and APES for estimation of spectral lines, *To appear in Circuits, Systems, and Signal Processing*, 2000.